

1 **Knockdown of Y-box-binding protein 2 induces**  
2 **mitochondrial dysfunction to interrupt zygotic genome**  
3 **activation in porcine embryos**

4 Wen-Jie Jiang <sup>1,2</sup>, Song-Hee Lee <sup>2</sup>, Hyeon-Ji Song <sup>2</sup>, Xiang-Shun Cui<sup>\*,2</sup>

5 1. College of Animal Science and Technology, Northeast Agricultural University, Harbin,  
6 150030, P. R. China

7 2. Department of Animal Science, Chungbuk National University, Cheongju, South Korea

8 \*Corresponding author

9  
10  
11  
12  
13  
14  
15  
16  
17  
18  
19  
20  
21  
22

ACCEPTED

## 23 **Abstract**

24 Y-box-binding protein 2 (YBX2) is a germ cell-specific protein that plays important roles  
25 in mRNA stability, transcription, and translation. However, the effects of YBX2 on porcine  
26 embryos development remain unclear. To investigate the function of YBX2 in early porcine  
27 embryonic development, YBX2 knockdown (KD) was performed via siRNA microinjection at  
28 the single-cell stage. The expression level of YBX2 gene was measured by quantitative real-  
29 time polymerase chain reaction (qRT-PCR). The effect of YBX2 on mitochondrial function and  
30 zygotic genome activation were detected by qRT-PCR, western blot, immunofluorescence  
31 staining. The results showed that YBX2 is essential for early embryonic development. YBX2  
32 KD decreased the blastocyst rate, mitochondrial activity, and the expression levels of NRF1,  
33 NRF2, and SIRT1, thereby reducing mitochondrial biogenesis. In addition, YBX2 KD led to an  
34 increase in maternal mRNA levels and a decrease in zygotic genome activation mRNA levels.  
35 However, maternal protein levels were reduced, indicating that YBX2 can affect the maternal-  
36 to-zygotic transition. Meanwhile, H3K9ac levels decreased and H3K9me3 levels increased  
37 following YBX2 KD, suggesting that YBX2 regulates gene transcription. YBX2 affected  
38 embryonic development by regulating mitochondrial biogenesis and ZGA expression.

39 **Keywords:** Y-box-binding protein 2, mitochondrial, zygotic genome activation, porcine  
40 embryos

## 41 **Introduction**

42 The fertilization of an oocyte with a spermatozoon is followed by a period of  
43 transcriptional quiescence of varying lengths when the embryonic genome contained in the

44 nucleus is not yet expressed. During this period of transcriptional silencing, development is  
45 driven by cytoplasmic factors that mainly consist of maternally deposited mRNA [1]. To ensure  
46 this developmental process, maternal mRNA activity is restricted to a precise time and space  
47 [1]. Translation is a major regulatory step in the translation of maternally stored mRNAs [2],  
48 suggesting that translation and post-translational regulation may play key roles in early  
49 embryogenesis. The maternal-to-zygotic transition (MZT) process includes zygotic genome  
50 activation (ZGA) [3]. According to previous studies, the major embryonic transcriptional  
51 activation of porcine ZGA occurs at the four-cell stage [4-6]. Moreover, the also regulation of  
52 genomic transcriptional activity during early embryonic development is governed by histone  
53 modifications, including processes like lysine acetylation and lysine methylation [7]. ZGA  
54 failure will causes abnormal embryonic development [4, 8].

55 Metabolic programming is closely related to early embryonic development, including  
56 ZGA. Mitochondria are one of the most important organelles in the cell and are responsible for  
57 metabolic, generating energy and participating in various physiological processes such as  
58 apoptosis [9, 10]. Mitochondrial tricarboxylic acid (TCA) cycle enzymes, which are normally  
59 located in the mitochondria, are also important for mouse ZGA [11]. During the two-cell stage,  
60 zygotic cells upregulated the expression of genes for pyruvate metabolism in mitochondria and  
61 oxidative phosphorylation[12]. Therefore, the mitochondria is crucial for ZGA.

62 Y-box-binding protein 2 (YBX2), alternatively referred to as MSY2, is a germ cell-  
63 specific Y-box-binding protein that is expressed in germ cells of the adult testis as well as in the  
64 developing fetal testis and ovary, but not in other normal tissues [13-15]. YBX2 is important

65 for round spermatids because it represses translational activity and transcript degradation [16],  
66 suggesting that YBX2 plays a role in regulating the translation of paternal mRNAs. Additionally,  
67 YBX2, which is specifically expressed in oocytes, is the most abundant RNA-binding protein  
68 (approximately 2% of total oocyte protein), and it is degraded at the 2-cell stage, which  
69 corresponds to the degradation cycle of maternal mRNAs in mouse[17]. Furthermore, the  
70 knockout/knockdown of the YBX2 can lead to a comprehensive reduction in mRNA within  
71 developing oocytes, thereby causing issues with oocyte maturation and early embryonic  
72 development [18, 19]. And, it has been shown that YBX2 stabilizes oocyte mRNA through  
73 reversible spongy cortical partitioning-dependent [20]. Thus, these findings suggest that YBX2  
74 plays a critical role in storing and stabilizing maternal mRNA and early embryonic development.  
75 Moreover, YBX2 stabilizes mRNA targets that encode proteins involved in mitochondrial  
76 function [21]. Based on this information, we investigated the impact of YBX2 on early porcine  
77 embryonic development.

78 In this study, the effects of YBX2 on the mitochondria, mRNA translation, and gene  
79 transcription were investigated using siRNA microinjection at the single-cell stage. These  
80 findings indicate that YBX2 plays a role in mitochondrial function and ZGA.

## 81 **Materials and Methods**

82 Unless specified otherwise, all chemicals were sourced from Sigma-Aldrich (St. Louis,  
83 MO, USA).

### 84 **2.1. Collection of porcine oocytes and in vitro maturation**

85 Ovaries from prepubertal gilts were obtained from a local abattoir (Farm Story Dodarm

86 B&F, Umsung, Chungbuk, Korea) and rinsed three times in saline solution containing 75  
87 mg/mL of penicillin G and 50 mg/mL of streptomycin sulfate at 37 °C. Follicles approximately  
88 3–6 mm in diameter were aspirated using a 10-mL disposable syringe. Selection criteria for the  
89 cumulus-oocyte complexes (COCs) included a minimum of three layers of compact cumulus  
90 cells. After three rinses with IVM [TCM-199 (11150-059; Gibco, Grand Island, NY, USA)  
91 supplemented with 100 mg/L sodium pyruvate, 10 ng/mL EGF, 10% (v/v) FF, 10 IU/mL LH,  
92 and 10 IU/mL FSH], approximately 70 COCs were placed into 4-well plates with 500 µL  
93 of IVM medium covered by mineral oil and cultured for 44 h at a temperature of 38.5 °C in an  
94 atmosphere containing 5% CO<sub>2</sub>.

## 95 **2.2. Parthenogenetic activation and *in vitro* culture**

96 The COCs were treated with 1 mg/mL hyaluronidase (Hy) and pipetted approximately 50  
97 times until the oocytes were naked and oocytes with the first polar bodies were selected. Next,  
98 two PDC of 110 V for 60 µs was applied to parthenogenetic activation of MII oocytes in 0.1  
99 mM CaCl<sub>2</sub>, 0.05 mM MgSO<sub>4</sub>, 0.01% PVA (w/v), and 0.5 mM HEPES. The activated oocytes  
100 were cultured in PZM-5 with 4 mg/mL BSA and 7.5 µg/mL cytochalasin B (CB) for 3 h.  
101 Subsequently, the oocytes underwent thorough washing and were then incubated in PZM-5  
102 medium added with 0.4% BSA for 6 days at 38.5 °C (5% CO<sub>2</sub>). The blastocyst (BL) rate was  
103 determined on day 6.

## 104 **2.3. Microinjection**

105 For knockdown (KD) experiments, small interfering RNAs (siRNAs) were crafted  
106 to target three distinct regions within the porcine genome (GenePharma, Shanghai, China). All

107 siRNA sequences used in this study are listed in Table 1. A mixture of YBX2-1, YBX2-2, and  
108 YBX2-3 siRNAs was prepared for microinjection. YBX2 siRNA (50  $\mu$ M) was microinjected  
109 into the cytoplasm of the zygotes using the Eppendorf Femto-Jet (Eppendorf, Hamburg,  
110 Germany) and Nikon Diaphot Eclipse TE300 inverted microscope (Nikon, Tokyo, Japan)  
111 equipped with the Narishige MM0-202N hydraulic 3-D micromanipulator (Narishige,  
112 Amityville, NY, USA). Following the injection, the embryos were nurtured in PZM-5 medium  
113 for either 2 or 6 days.

#### 114 **2.4. Immunofluorescence staining**

115 Embryos were fixed using a 3.7% solution of paraformaldehyde (PFA) for 30 min at room  
116 temperature (RT), followed by three washing with PVA/PBS. Subsequently, they were  
117 permeabilized with 1% Triton X-100 for 30 min and blocked with a solution of 3.0% BSA with  
118 0.1% Triton X-100 for 1 hour at RT. Embryos were incubated overnight at 4 °C with different  
119 primary antibodies. After washing three times with PVA/PBS, the embryos were treated with  
120 different second antibodies (1:200; A10040; Invitrogen) for 1 h at RT. The embryos were then  
121 mounted onto slides using Vectashield mounting medium with DAPI (Vector Laboratories,  
122 Burlingame, CA, USA) and visualized using a confocal microscope (Zeiss LSM 710 META;  
123 Zeiss, Germany). The resulting images were processed with Zen software version 8.0 (Zeiss).

#### 124 **2.5. MitoTracker staining**

125 Embryos were treated with MitoTracker Red CMXRos at a concentration of 500 nM  
126 (M7512; Invitrogen) for a duration of 30 min at a temperature of 38.5°C. Post-incubation, they  
127 were washed thrice with PVA/PBS. Subsequently, the embryos were fixed in 3.7% PFA for 30

128 min at RT and washed an additional three times with PVA/PBS. Finally, the embryos were  
129 mounted onto slides.

## 130 **2.6. Real-time reverse transcription-quantitative polymerase chain reaction (RT-qPCR)**

131 mRNA was isolated from 30 embryos from the control and YBX2 KD groups respectively,  
132 utilizing the DynaBeads mRNA Direct Kit (61012; Thermo Fisher Scientific, Waltham, MA,  
133 USA), following the protocol provided by the manufacturer. The RNA was converted into  
134 cDNA using oligo (dT) 20 primers and SuperScript III Reverse Transcriptase (Thermo Fisher  
135 Scientific). For RT-qPCR, the WizPure qPCR Master Kit was utilized. A 20  $\mu$ L reaction mixture  
136 was prepared, consisting of 10  $\mu$ L SYBR Green, 1  $\mu$ L each of the forward and reverse primers,  
137 2  $\mu$ L of cDNA, and 7  $\mu$ L of double distilled water (ddH<sub>2</sub>O). The amplification cycle was set as  
138 follows: 95 °C for 3 min, followed by 40 cycles of 95 °C for 15 s, 60 °C for 25 s, 72 °C for 10  
139 s, and a final extension at 72 °C for 5 min. The 18S rRNA gene served as reference gene. The  
140 primer sequences for each target gene are detailed in Table 2. mRNA quantification was  
141 calculated using the  $2^{-\Delta\Delta C_t}$  method.

## 142 **2.7. Protein extraction and western blot analysis**

143 Sixty embryos each from the control and YBX2 KD groups were combined with 20  $\mu$ L of  
144 ice-cold Laemmli sample buffer (sodium dodecyl sulfate [SDS] sample buffer that includes 2-  
145 mercaptoethanol) and heated at 95 °C for 10 min. The proteins from each sample were then  
146 separated by 10% SDS-polyacrylamide gel electrophoresis and transferred to a polyvinylidene  
147 fluoride (PVDF) membrane (Millipore, Bedford, MA, USA). To prevent nonspecific binding,  
148 the membranes were blocked with Tris-buffered saline with Tween-20 (TBST), supplemented

149 with either 5% skim milk powder or bovine serum albumin (BSA), for 1 h at RT . Subsequently,  
150 the membranes were incubated with different primary antibodies in a blocking solution  
151 overnight at 4 °C. After washing three times with TBST (10 min each), the membranes were  
152 treated with secondary antibodies (1:20000) for 1 h at RT. The membranes were subsequently  
153 developed using the SuperSignal West Femto Maximum Sensitivity Substrate (Thermo Fisher  
154 Scientific). The resulting band intensities were quantified using ImageJ software.

## 155 **2.8. Statistical analysis**

156 Each experiment was performed at least in triplicate. Data were analyzed using the  
157 GraphPad Prism 5 software (GraphPad). Statistical analysis was performed by t-test between  
158 control and YBX2 KD group. All data are shown as the mean  $\pm$  standard error of mean (SEM).  
159 Statistical significance was set at  $p < 0.05$ .

# 160 **Results**

## 161 **3.1. The expression of YBX2 during embryo development**

162 To ascertain the subcellular distribution of YBX2 during embryonic development,  
163 immunofluorescence staining was conducted to delineate its location in two-cell (2C; n = 10),  
164 four-cell (4C; n = 10), and BL (n = 10) embryos. As shown in Fig. 1A, YBX2 is localized in  
165 the nucleus, cytoplasm and cortex during the 2C and 4C stages. However, it was localized  
166 in the cytoplasm at the BL stage. Next, we determined the protein expression levels of YBX2  
167 by western blotting, the result indicated that YBX2 was present during porcine embryonic  
168 development (Fig. 1B). Subsequently, using RT-qPCR, we observed that the mRNA levels of  
169 YBX2 were the highest at the 2C stage and decreased at the 4C stage (Fig. 1C).



### 170 **3.2. Effects of YBX2 on early porcine embryonic development**

171 To study the effects of YBX2 on porcine embryonic development, YBX2 (YBX2 KD)  
172 siRNA was microinjected into the zygote. YBX2 KD resulted in a significant decrease in  
173 mRNA levels at the 4C stage (1 vs.  $0.15 \pm 0.06$ ;  $p < 0.01$ ; Fig. 2A). Western blotting also  
174 demonstrated that YBX2 protein expression levels were reduced (1 vs.  $0.83 \pm 0.02$ ;  $p < 0.05$ ;  
175 Fig. 2B and C). Upon YBX2 KD, the BL formation rate in the YBX2 KD group was  
176 significantly lower than that in the control group ( $34.81 \pm 2.86$  vs.  $17.74 \pm 3.69$ ;  $p < 0.05$ ; Fig.  
177 2D), indicating that YBX2 plays an important role in embryo development.

### 178 **3.3. Effects of YBX2 on mitochondrial biogenesis**

179 YBX2 stabilizes mRNA targets that encode proteins rich in mitochondrial function. To  
180 determine mitochondrial activity, embryos were stained with MitoTracker Red CMXRos at the  
181 4C stage. As shown in Fig. 3A and B, the intensity of active mitochondria was significantly  
182 decreased after YBX2 KD ( $1.01 \pm 0.02$  vs.  $0.76 \pm 0.03$ ;  $p < 0.001$ ). PGC1 $\alpha$ , SIRT1, NRF1, and  
183 NRF2 impact mitochondrial biogenesis. At the 4C stage, immunofluorescence staining revealed  
184 that NRF2 expression levels were significantly reduced upon YBX2 KD ( $1 \pm 0.02$  vs.  $0.68 \pm$   
185  $0.02$ ;  $p < 0.001$ ; Fig. 3C and D). Western blotting revealed a reduction in the protein levels of  
186 SIRT1 (1 vs.  $0.79 \pm 0.04$ ;  $p < 0.05$ ; Fig. 3E) and NRF1 (1 vs.  $0.75 \pm 0.04$ ;  $p < 0.05$ ; Fig. 3E)  
187 upon YBX2 KD. Taken together, these results indicate that YBX2 KD impairs mitochondrial  
188 biogenesis.

### 189 **3.4. Effects of YBX2 on ZGA**

190 Mitochondrial dysfunction can affect ZGA during early embryonic development [3, 22].

191 Therefore, we investigated the effects of YBX2 on ZGA. Initially, we detected maternal mRNA  
192 degradation and ZGA gene expression using RT-qPCR in the control and YBX2 KD groups. As  
193 shown in Fig. 4A, the maternal expression levels of *GDF9* ( $p < 0.05$ ), *BMP15* ( $p < 0.05$ ), and  
194 *CCNB1* ( $p < 0.05$ ) in the YBX2 KD group was significantly higher than those in the control  
195 group. However, there was no significant difference in *MOS* mRNA levels between YBX2 KD  
196 and control groups. In addition, the protein levels of CCNB1 ( $0.81 \pm 0.02$  vs. 1;  $p < 0.05$ ; Fig.  
197 4B and C) and BMP15 ( $0.69 \pm 0.01$  vs. 1;  $p < 0.01$ ; Fig. 4B and C) were significantly lower in  
198 the YBX2 KD group compared to the control group. ZGA genes *ZSCAN4* ( $0.64 \pm 0.01$  vs. 1;  
199  $p < 0.01$ ; Fig. 4D) and *DPPA2* ( $0.58 \pm 0.05$  vs. 1;  $p < 0.01$ ; Fig. 4D) expression levels were  
200 significantly decreased after YBX2 KD. These data indicate that YBX2 KD impairs the ZGA  
201 process.

### 202 **3.5. Effects of YBX2 on histone modifications**

203 Histone modifications occur throughout the early embryonic development and affect the  
204 interactions between transcriptional factors and chromatin. Any irregularities in histone  
205 modifications may cause developmental abnormalities in embryos. Therefore, we examined the  
206 effect of YBX2 on H3K9ac and H3K9me3 levels. The result showed that the levels of  
207 H3K9me3 in the YBX2 KD group was significantly higher than those in the control group ( $1 \pm$   
208  $0.00$  vs.  $1.25 \pm 0.03$ ;  $p < 0.05$ ; Fig. 5A and B). Moreover, western blotting for H3K9ac was also  
209 decreased in the YBX2 KD group ( $1$  vs.  $0.56 \pm 0.10$ ;  $p < 0.05$ ; Fig. 5C and D). These results  
210 indicate that YBX2 affects gene transcription.

211

## **Discussion**

212 We investigated the function of YBX2 in early porcine embryonic development (Fig. 6).  
213 These findings indicated that YBX2 is a maternal gene with important roles in mitochondrial  
214 biogenesis and ZGA in porcine embryos. YBX2 KD resulted in mitochondrial dysfunction and  
215 anomalies in the ZGA process, leading to abnormal porcine embryonic development.

216 Bovine embryos revealed that the protein expression levels of YBX2 are analogous to that  
217 in mice, with higher abundance at the early cleavage stage and a subsequent decline after the  
218 MZT [17, 23], suggesting that YBX2 is prevalent in early embryos. In this study, YBX2 mRNA  
219 and protein expression patterns similar to those in bovine were observed in porcine embryos.  
220 Depending on its expression profile, YBX2 prevents premature translation of mRNAs in early  
221 embryos. Since porcine embryos at the morula stage and bovine embryos at the 16-cell stage  
222 can transcribe their own mRNAs they do not require YBX2, suggesting that YBX2 is a maternal  
223 gene that plays a crucial role before the start of embryonic transcription. In addition, lack of  
224 YBX2 in mouse oocytes interferes with oocyte growth and maturation, RNA stability, and the  
225 transcriptome, resulting in reduced fertility [18, 19]. In the current study, YBX2 KD decreased  
226 the BL formation rate, suggesting that YBX2 plays a crucial role in embryo development.  
227 Furthermore, numerous studies have shown that deletion of YBX2 leads to spermatogenic arrest  
228 [24, 25]. In summary, YBX2 is important in oocyte, sperm, and early embryonic development.

229 YBX2 stabilizes mRNA targets encoding proteins rich in mitochondrial function, such as  
230 PGC1 $\alpha$ , which can affect mitochondrial activity [21]. PGC1 $\alpha$  acts as a key regulator of  
231 mitochondrial biogenesis and it has been shown that PGC1 $\alpha$  degradation inhibits mitochondrial  
232 biogenesis [26, 27]. Activated PGC1 $\alpha$  leads to increased expression levels of NRF1 and NRF2

233 [26]. NRF2 affects mitochondrial membrane potential, which is a universal indicator of  
234 mitochondrial health and cellular metabolism [21]. Additionally, Nrf2 deficiency results in  
235 impaired mitochondrial function (mitochondrial depolarization, reduced ATP levels ) [28].  
236 SIRT1 is another marker of mitochondrial function and activation of the SIRT1/PGC-1 $\alpha$  axis  
237 prevents aberrant mitochondrial fission [29]. In the present study, YBX2 KD decreased  
238 mitochondrial activity and expression levels of NRF1, NRF2, PGC1 $\alpha$ , and SIRT1, indicating  
239 that YBX2 KD impaired mitochondrial biogenesis.

240 Additionally, mitochondrial dysfunction can affect ZGA during early embryonic  
241 development [3, 22]. Furthermore, mitochondrial metabolism has a profound effect on histone  
242 modifications required for gene expression [30]. Therefore, impairment of mitochondrial  
243 function caused by YBX2 KD may also affect ZGA. During ZGA, the gradual degradation of  
244 most maternal factors is essential for the proper progression of embryonic development. Failure  
245 to degrade these maternal factors can result in developmental issues within the embryo [31]. In  
246 the present study, YBX2 KD resulted in a significant increase in maternal mRNA expression  
247 levels and a decrease in protein expression levels, suggesting that maternal gene degradation  
248 and translation were disrupted. Moreover, *ZSCAN4* and *DPPA2* are ZGA markers [32, 33].  
249 Studies have reported that either *Zscan4* KD or its overexpression impairs early embryonic  
250 development [34]. *DPPA2* and *DPPA4* are positive regulators of 2C-like cells and ZGA gene  
251 transcription [32]. Upon YBX2 KD, we observed a significant reduction in the mRNA levels  
252 of both *ZSCAN4* and *DPPA2*, suggesting that YBX2 can affect ZGA. Regulation of ZGA is  
253 influenced by histone modifications, including H3K9ac and H3K9me3. H3K9me3 is associated

254 with constitutive heterochromatin formation and repression of genes transcription [35].  
255 H3K9ac is associated with gene transcription activation. In general, gene activation implies that  
256 chromatin shifts to an open state; in gene-regulated regions, active markers are enriched and  
257 repressive markers disappear [4, 36, 37]. YBX2 KD increased H3K9me3 levels, whereas  
258 H3K9ac levels were reduced, indicating the repression of gene transcription. Taken together,  
259 these results indicated that YBX2 regulates the ZGA process during embryonic development in  
260 pigs.

261 In conclusion, the current study showed that YBX2 KD decreased mitochondrial  
262 biogenesis, reduced transcriptional activity, and caused abnormal histone modifications to  
263 impair ZGA. Our research provides insights into the mechanism through which YBX2  
264 modulates the developmental capacity of embryos *in vitro*, and opens avenues for developing  
265 strategies to enhance embryonic viability and potentially improve assisted reproductive  
266 technologies.

267

268

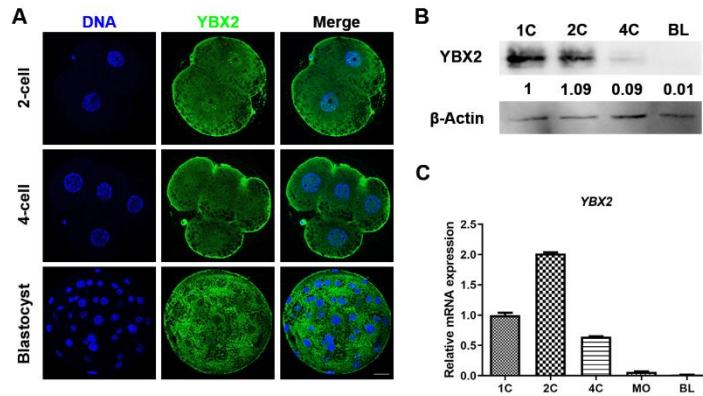
## References

- 270 1. Winata CL, Korzh V. The translational regulation of maternal mRNAs in time and space. *FEBS*  
271 *Lett.* 2018;592(17):3007-23.
- 272 2. Teixeira FK, Lehmann R. Translational Control during Developmental Transitions. *Cold Spring*  
273 *Harb Perspect Biol.* 2019;11(6).
- 274 3. Wu SL, Ju JQ, Ji YM, Zhang HL, Zou YJ, Sun SC. Exposure to acrylamide induces zygotic genome  
275 activation defects of mouse embryos. *Food Chem Toxicol.* 2023;175:113753.
- 276 4. Li XH, Sun MH, Jiang WJ, Zhou D, Lee SH, Heo G, et al. ZSCAN4 Regulates Zygotic Genome  
277 Activation and Telomere Elongation in Porcine Parthenogenetic Embryos. *Int J Mol Sci.*  
278 2023;24(15).
- 279 5. Zhou W, Nie ZW, Zhou DJ, Cui XS. Acetyl-CoA synthases are essential for maintaining histone  
280 acetylation under metabolic stress during zygotic genome activation in pigs. *Journal of cellular*  
281 *physiology.* 2021;236(10):6948-62.
- 282 6. Zhou W, Niu YJ, Nie ZW, Kim JY, Xu YN, Yan CG, et al. Nuclear accumulation of pyruvate  
283 dehydrogenase alpha 1 promotes histone acetylation and is essential for zygotic genome activation  
284 in porcine embryos. *Biochimica et biophysica acta Molecular cell research.* 2020;1867(4):118648.
- 285 7. Fu X, Zhang C, Zhang Y. Epigenetic regulation of mouse preimplantation embryo development.  
286 *Curr Opin Genet Dev.* 2020;64:13-20.
- 287 8. Xue L, Cai JY, Ma J, Huang Z, Guo MX, Fu LZ, et al. Global expression profiling reveals genetic  
288 programs underlying the developmental divergence between mouse and human embryogenesis.  
289 *BMC Genomics.* 2013;14:568.
- 290 9. Niu YJ, Zhou W, Nie ZW, Shin KT, Cui XS. Melatonin enhances mitochondrial biogenesis and  
291 protects against rotenone-induced mitochondrial deficiency in early porcine embryos. *J Pineal Res.*  
292 2020;68(2):e12627.
- 293 10. Mou C, Wang Y, Pan S, Shi K, Chen Z. Porcine sapelovirus 2A protein induces mitochondrial-  
294 dependent apoptosis. *Front Immunol.* 2022;13:1050354.
- 295 11. Nagaraj R, Sharpley MS, Chi F, Braas D, Zhou Y, Kim R, et al. Nuclear Localization of  
296 Mitochondrial TCA Cycle Enzymes as a Critical Step in Mammalian Zygotic Genome Activation.  
297 *Cell.* 2017;168(1-2):210-23.e11.
- 298 12. Sun H, Zhang Z, Li T, Li T, Chen W, Pan T, et al. Live-cell imaging reveals redox metabolic  
299 reprogramming during zygotic genome activation. *Journal of cellular physiology.*  
300 2023;238(9):2039-49.
- 301 13. Kohno Y, Matsuki Y, Tanimoto A, Izumi H, Uchiumi T, Kohno K, et al. Expression of Y-box-binding

- 302 protein dbpC/contrin, a potentially new cancer/testis antigen. *Br J Cancer*. 2006;94(5):710-6.
- 303 14. Tekur S, Pawlak A, Guellaen G, Hecht NB. Contrin, the human homologue of a germ-cell Y-box-  
304 binding protein: cloning, expression, and chromosomal localization. *J Androl*. 1999;20(1):135-44.
- 305 15. Suzuki I, Yoshida S, Tabu K, Kusunoki S, Matsumura Y, Izumi H, et al. YBX2 and cancer testis  
306 antigen 45 contribute to stemness, chemoresistance and a high degree of malignancy in human  
307 endometrial cancer. *Sci Rep*. 2021;11(1):4220.
- 308 16. Kleene KC. Position-dependent interactions of Y-box protein 2 (YBX2) with mRNA enable mRNA  
309 storage in round spermatids by repressing mRNA translation and blocking translation-dependent  
310 mRNA decay. *Mol Reprod Dev*. 2016;83(3):190-207.
- 311 17. Yu J, Hecht NB, Schultz RM. Expression of MSY2 in mouse oocytes and preimplantation embryos.  
312 *Biology of reproduction*. 2001;65(4):1260-70.
- 313 18. Yu J, Deng M, Medvedev S, Yang J, Hecht NB, Schultz RM. Transgenic RNAi-mediated reduction  
314 of MSY2 in mouse oocytes results in reduced fertility. *Developmental biology*. 2004;268(1):195-  
315 206.
- 316 19. Medvedev S, Pan H, Schultz RM. Absence of MSY2 in mouse oocytes perturbs oocyte growth and  
317 maturation, RNA stability, and the transcriptome. *Biology of reproduction*. 2011;85(3):575-83.
- 318 20. Zhang Z, Liu R, Zhou H, Luo Y, Mu J, Fu J, et al. YBX2-dependent stabilization of oocyte mRNA  
319 through a reversible sponge-like cortical partition. *Cell research*. 2023;33(8):640-3.
- 320 21. Xu D, Xu S, Kyaw AMM, Lim YC, Chia SY, Chee Siang DT, et al. RNA Binding Protein Ybx2  
321 Regulates RNA Stability During Cold-Induced Brown Fat Activation. *Diabetes*. 2017;66(12):2987-  
322 3000.
- 323 22. Li Y, Mei NH, Cheng GP, Yang J, Zhou LQ. Inhibition of DRP1 Impedes Zygotic Genome  
324 Activation and Preimplantation Development in Mice. *Front Cell Dev Biol*. 2021;9:788512.
- 325 23. Vigneault C, McGraw S, Sirard MA. Spatiotemporal expression of transcriptional regulators in  
326 concert with the maternal-to-embryonic transition during bovine in vitro embryogenesis.  
327 *Reproduction*. 2009;137(1):13-21.
- 328 24. Yang J, Morales CR, Medvedev S, Schultz RM, Hecht NB. In the absence of the mouse DNA/RNA-  
329 binding protein MSY2, messenger RNA instability leads to spermatogenic arrest. *Biol Reprod*.  
330 2007;76(1):48-54.
- 331 25. Yang J, Medvedev S, Yu J, Tang LC, Agno JE, Matzuk MM, et al. Absence of the DNA-/RNA-  
332 binding protein MSY2 results in male and female infertility. *Proc Natl Acad Sci U S A*.  
333 2005;102(16):5755-60.
- 334 26. Chen L, Qin Y, Liu B, Gao M, Li A, Li X, et al. PGC-1 $\alpha$ -Mediated Mitochondrial Quality Control:

- 335 Molecular Mechanisms and Implications for Heart Failure. *Front Cell Dev Biol.* 2022;10:871357.
- 336 27. Zhao M, Li Y, Lu C, Ding F, Xu M, Ge X, et al. PGC1 $\alpha$  Degradation Suppresses Mitochondrial  
337 Biogenesis to Confer Radiation Resistance in Glioma. *Cancer research.* 2023;83(7):1094-110.
- 338 28. Holmström KM, Baird L, Zhang Y, Hargreaves I, Chalasani A, Land JM, et al. Nrf2 impacts cellular  
339 bioenergetics by controlling substrate availability for mitochondrial respiration. *Biology open.*  
340 2013;2(8):761-70.
- 341 29. Su X, Li Q, Yang M, Zhang W, Liu X, Ba Y, et al. Resveratrol protects against a high-fat diet-  
342 induced neuroinflammation by suppressing mitochondrial fission via targeting SIRT1/PGC-1 $\alpha$ .  
343 *Experimental neurology.* 2024;380:114899.
- 344 30. Martinez-Pastor B, Cosentino C, Mostoslavsky R. A tale of metabolites: the cross-talk between  
345 chromatin and energy metabolism. *Cancer Discov.* 2013;3(5):497-501.
- 346 31. Sha QQ, Zheng W, Wu YW, Li S, Guo L, Zhang S, et al. Dynamics and clinical relevance of maternal  
347 mRNA clearance during the oocyte-to-embryo transition in humans. *Nat Commun.*  
348 2020;11(1):4917.
- 349 32. Eckersley-Maslin M, Alda-Catalinas C, Blotenburg M, Kreibich E, Krueger C, Reik W. Dppa2 and  
350 Dppa4 directly regulate the Dux-driven zygotic transcriptional program. *Genes Dev.* 2019;33(3-  
351 4):194-208.
- 352 33. Takahashi K, Ross PJ, Sawai K. The necessity of ZSCAN4 for preimplantation development and  
353 gene expression of bovine embryos. *J Reprod Dev.* 2019;65(4):319-26.
- 354 34. Falco G, Lee SL, Stanghellini I, Bassey UC, Hamatani T, Ko MS. Zscan4: a novel gene expressed  
355 exclusively in late 2-cell embryos and embryonic stem cells. *Dev Biol.* 2007;307(2):539-50.
- 356 35. Zhou C, Halstead MM, Bonnet-Garnier A, Schultz RM, Ross PJ. Resetting H3K4me3, H3K27ac,  
357 H3K9me3 and H3K27me3 during the maternal-to-zygotic transition and blastocyst lineage  
358 specification in bovine embryos. *bioRxiv.* 2022:2022.04.07.486777.
- 359 36. Karlić R, Chung HR, Lasserre J, Vlahovicek K, Vingron M. Histone modification levels are  
360 predictive for gene expression. *Proc Natl Acad Sci U S A.* 2010;107(7):2926-31.
- 361 37. Sun MH, Jiang WJ, Li XH, Lee SH, Heo G, Zhou D, et al. ATF7-dependent epigenetic changes  
362 induced by high temperature during early porcine embryonic development. *Cell Prolif.*  
363 2023;56(2):e13352.





365

366

**Table 1 Information of siRNA for Microinjection**

siRNA	siRNA sequences
siYBX2-1	F: GUUCACCAGACAGCUAUUATT R: UAAUAGCUGUCUGGUGAACTT
siYBX2-2	F: GAAGCUGCUAACGUAACUGTT R: CAGUUACGUUAGCAGCUUCTT
siYBX2-3	F: GGUAGAACCCAAAGAGACATT R: UGUCUCUUUGGGUUCUACCTT

367

368

369

370  
371  
372

**Table 2 Information of Primers Used for RT-PCR**

<b>Genes</b>	<b>Primer sequences</b>	<b>Accession No.</b>	<b>Product size (bp)</b>
<i>YBX2</i>	F: CAAGTCCTGGGCACTGTCAA R: CAGGCCCAGTTACGTTAGCA	XM_021067811.1	214
<i>DPPA2</i>	F: TACAGAAGGTTGGGTTTCGCC R: GGTCTGGGGATGGGAAAGTG	XM_003358822.4	116
<i>ZSCAN4</i>	F: CTTGTTTGGTCCTCGAACAGT R: TTCATGCCATCGTCTGTCAGGT	XM_021097584.1	130
<i>CCNB1</i>	F: CCAACTGGTTGGTGTCACTG R: GCTCTCCGAAGAAAATGCAG	NM_001170768.1	195
<i>BMP15</i>	F: CCCTCGGGTACTACACTATG R: GGCTGGGCAATCATATCC	NM_001005155.2	192
<i>GDF9</i>	F: GAGCTCAGGACACTGTAAGCT R: CTTCTCGTGGATGATGTTCTG	NM_001001909.1	272
<i>MOS</i>	F: TGGGAAGAACTGGAGGACA R: TTCGGGTCAGCCCAGGTTCA	NM_001113219.1	121
<i>18S</i>	F: CGCGGTTCTATTTTGTGGT R: AGTCGGCATCGTTTATGGTC	NR_046261	219

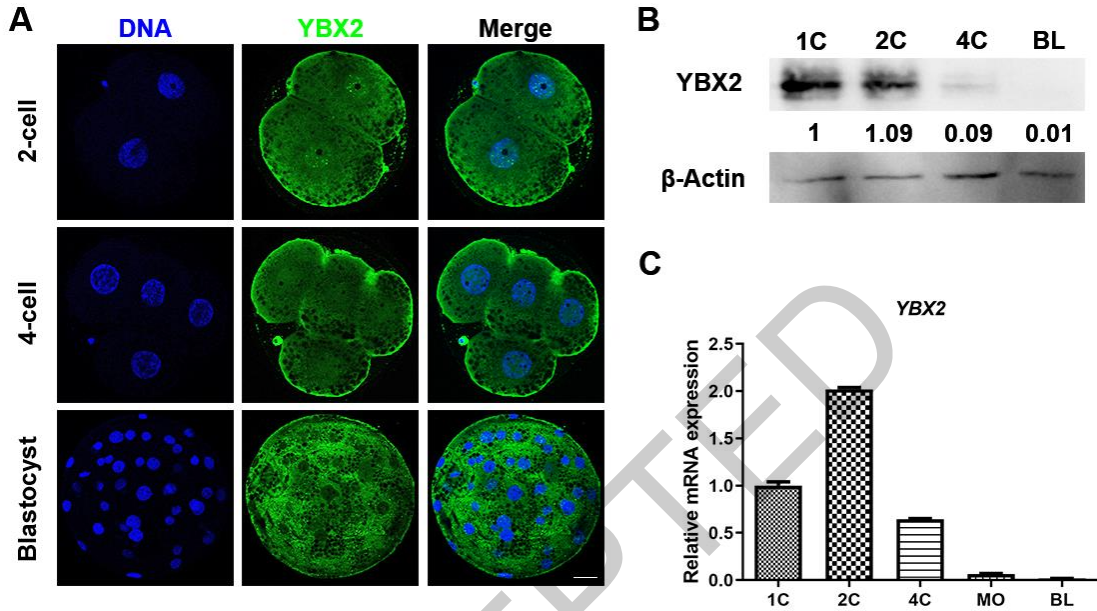
373  
374  
375

376

377

378 **Figure captions**

379



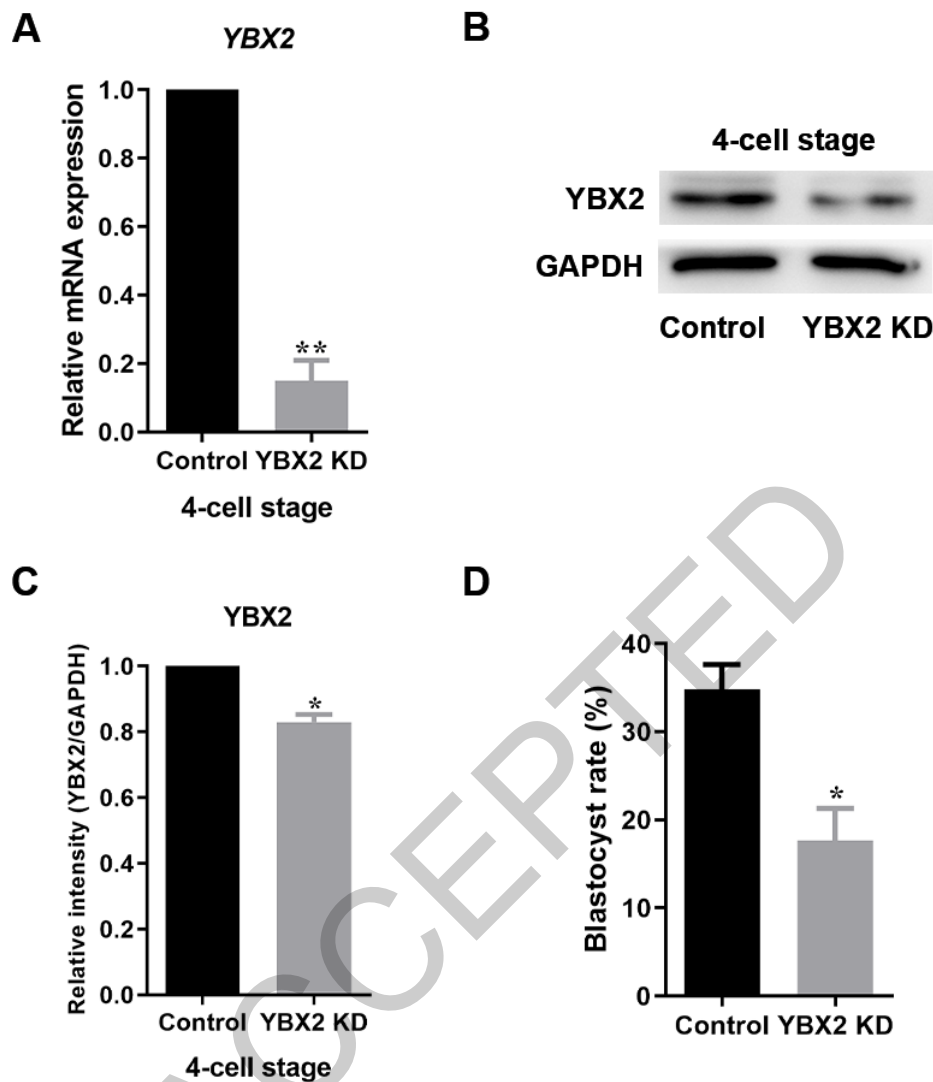
380

381

382 **Fig. 1 The expression of YBX2 during embryo development.** A. Immunofluorescence  
383 images for YBX2 localization at two-cell (2C), four-cell (4C), and blastocyst (BL) stages. Blue:  
384 DNA; green: YBX2. Scale bar: 40  $\mu$ m. B. RT-qPCR results of YBX2 mRNA expression  
385 relative to its expression in single-cell stage. C. Western blotting results of YBX2 protein  
386 expression at 1C, 2C, 4C, and BL stages.

387

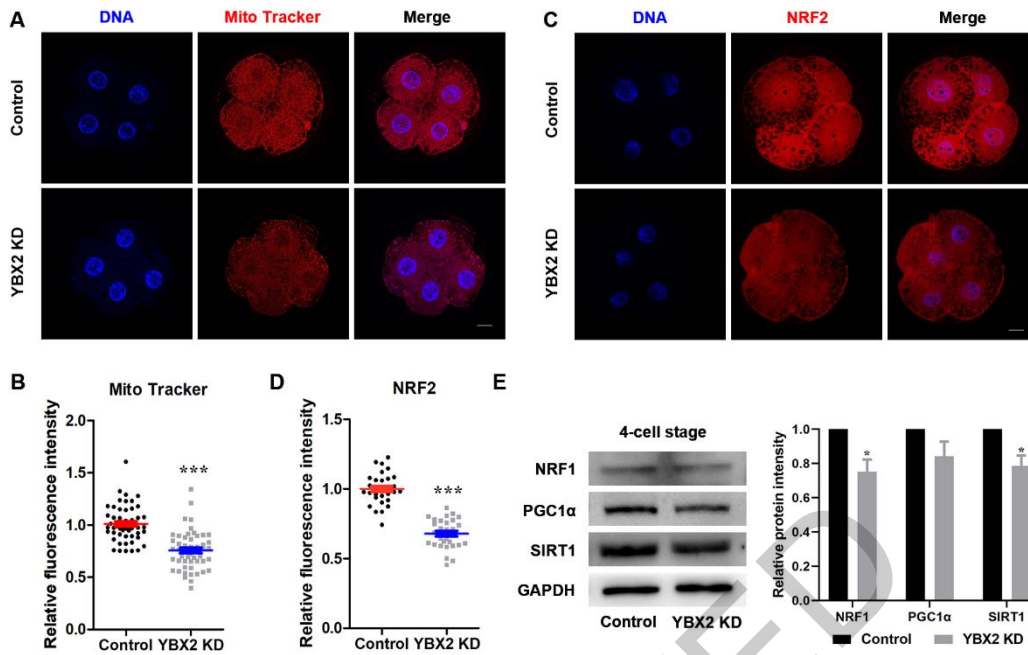
388



390

391 **Fig. 2 Effects of YBX2 on early porcine embryonic development.** A. RT-qPCR results of392 *YBX2* mRNA expression levels in 4C stage embryos of control and *YBX2* knockdown (KD)393 groups. Compared with the control group, the expression level of *YBX2* mRNA was394 significantly lower in the *YBX2* KD group. \*\* $p < 0.01$ . B. Western blotting images of *YBX2*395 protein expression levels in control and *YBX2* KD groups. C. Relative *YBX2* protein expression396 levels in 4C stage embryos of control and *YBX2* KD groups. *YBX2* protein expression397 decreased significantly in the *YBX2* KD group. \* $p < 0.05$ . D. Blastocyst rate after *YBX2* KD.398 The blastocyst rate reduced significantly in the *YBX2* KD group. \* $p < 0.05$ .

399

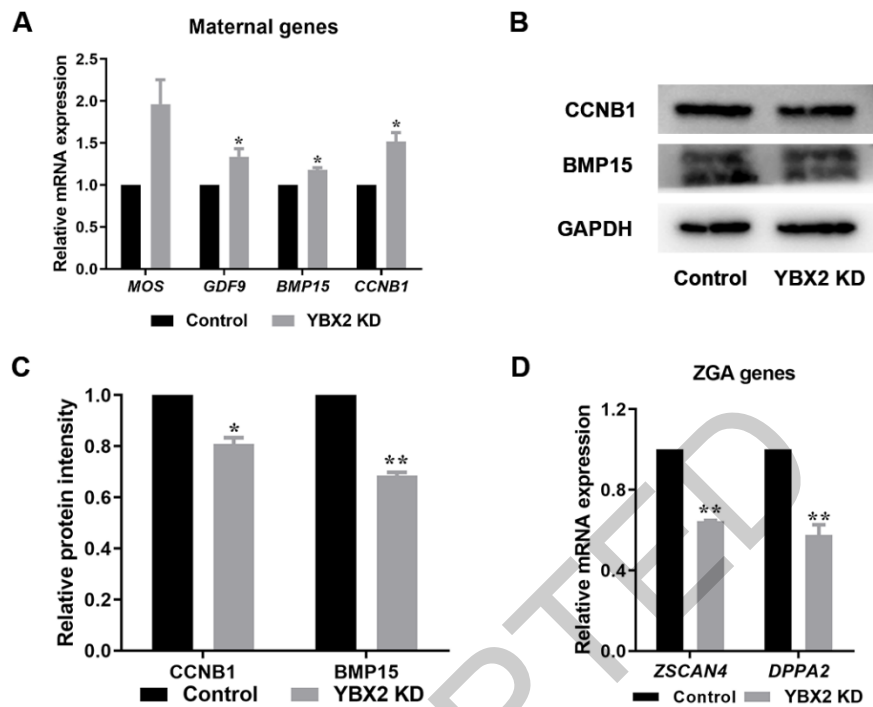


401

402 **Fig. 3 Effects of YBX2 on mitochondrial biogenesis.** A. Immunofluorescence images of Mito  
 403 Tracker at 4C stage after *YBX2* knockdown (KD). Blue: DNA; Red: Mito Tracker. Scale bar:  
 404 20  $\mu$ m. B. Relative fluorescence intensity of Mito Tracker. Compared with the control group,  
 405 Mito Tracker fluorescence intensity of 4C in the *YBX2* KD group was significantly lower. \*\*\* $p$   
 406  $< 0.001$ . C. Immunofluorescence images of NRF2 at the 4C stage after *YBX2* KD. Blue:  
 407 DNA; Red: NRF2; Scale bar: 20  $\mu$ m. D. Relative fluorescence intensity of NRF2. Compared  
 408 with the control group, NRF2 fluorescence intensity of 4C in the *YBX2* KD group was  
 409 significantly lower. \*\*\* $p < 0.001$ . E. Western blotting images of protein expression levels  
 410 after *YBX2* KD. NRF1 and SIRT1 protein expression were significantly decreased in the *YBX2*  
 411 KD group. \* $p < 0.05$ .

412

413

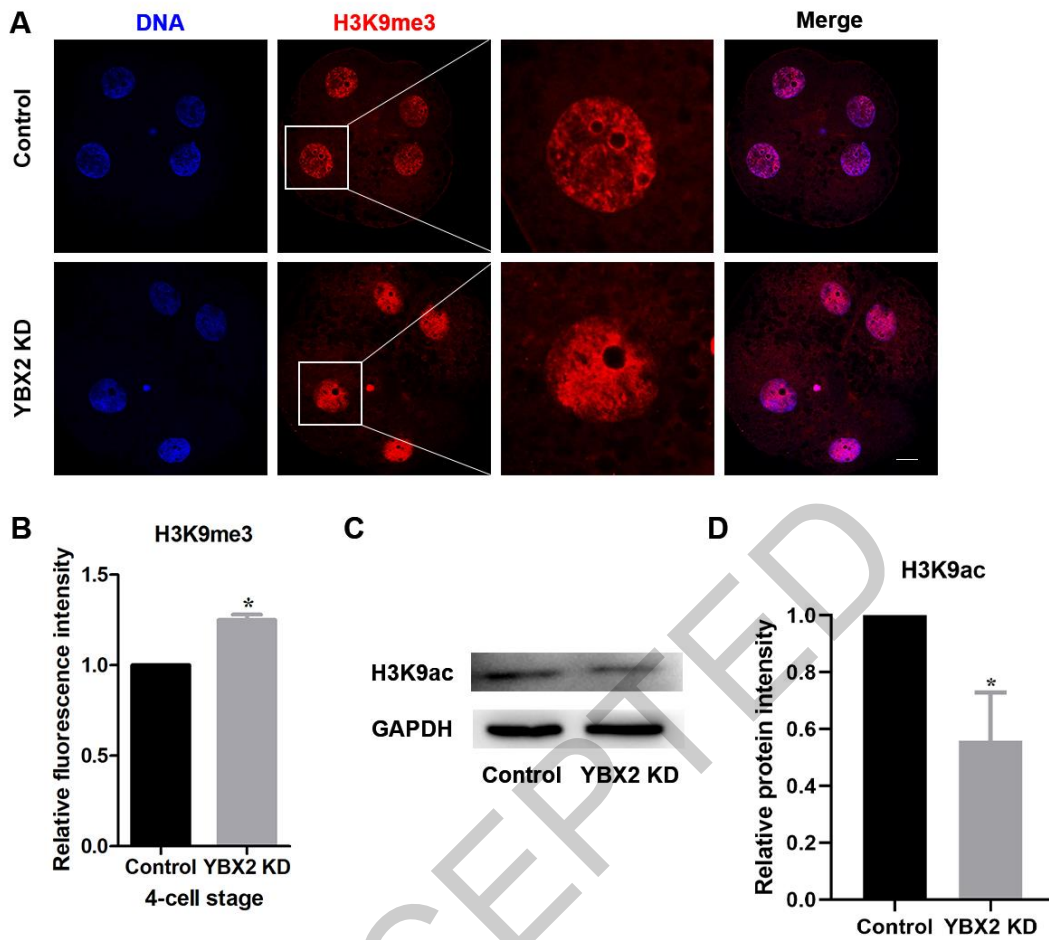


415

416 **Fig. 4 Effects of YBX2 on ZGA.** A. Relative mRNA expression of maternal genes (*MOS*,  
 417 *GDF9*, *BMP15*, and *CCNB1*) at 4C stage after YBX2 knockdown (KD). Compared with the  
 418 control group, the expression levels of *GDF9*, *BMP15* and *CCNB1* mRNA were significantly  
 419 higher in the YBX2 KD group. \* $p < 0.05$ . B. Western blotting images of CCNB1 and BMP15  
 420 after YBX2 KD. C. Relative protein levels of CCNB1 and BMP15 after YBX2 KD. CCNB1 and  
 421 BMP15 protein expression were significantly decreased in the YBX2 KD group. \* $p < 0.05$ ; \*\* $p$   
 422  $< 0.01$ . D. Relative mRNA expression levels of ZGA genes (*ZSCAN4* and *DPPA2*) at 4C stage  
 423 after YBX2 KD. Compared with the control group, the expression levels of *ZSCAN4* and *DPPA2*  
 424 mRNA were significantly lower in the YBX2 KD group. \*\* $p < 0.01$ .

425

426

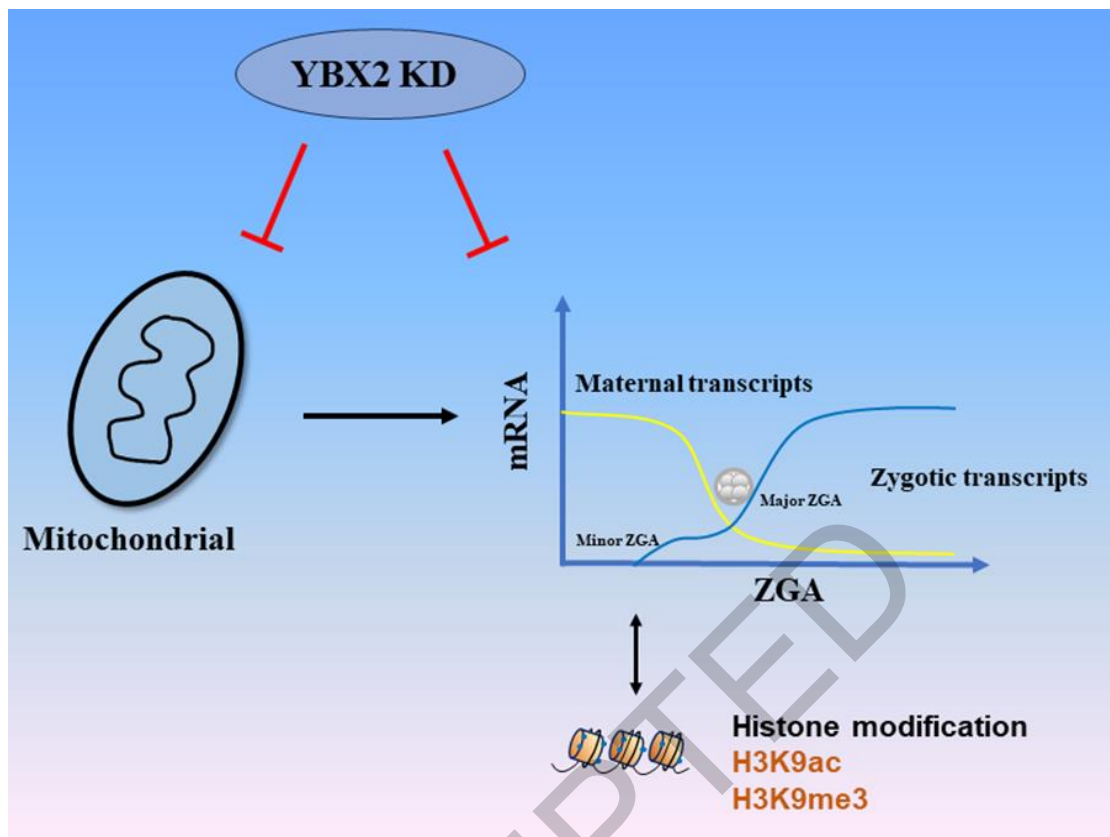


428

429 **Fig. 5 Effects of YBX2 on histone modifications.** A. Immunofluorescence images of  
 430 H3K9me3 at four-cell (4C) stage. Blue: DNA; Red: H3K9me3. Scale bar: 20  $\mu$ m. B. Relative  
 431 fluorescence intensity of H3K9me3 at 4C stage after YBX2 knockdown (KD). Compared with  
 432 the control group, H3K9me3 fluorescence intensity of 4C in the YBX2 KD group was  
 433 significantly higher. \* $p < 0.05$ . C. Protein expression level of H3K9ac at 4C stage after YBX2  
 434 KD. D. Protein level of H3K9ac at 4C stage after YBX2 KD. H3K9ac protein expression was  
 435 significantly decreased in the YBX2 KD group. \* $p < 0.05$ .

436

437



439

440 **Fig. 6 Schematic representation depicting functions of YBX2 in porcine embryos. YBX2**

441 knockdown induces mitochondrial dysfunction to regulate zygotic genome activation (ZGA).

442 YBX2 affects maternal gene translation and promotes transcription by regulating histone

443 acetylation (H3K9ac) and methylation (H3K9me3) in porcine ZGA.

444